

Nitrogen Doping of Ceria

A. Belén Jorge,[†] Jordi Fraxedas,^{†,‡} Andrés Cantarero,[§] Anthony J. Williams,^{||} Jennifer Rodgers,^{||} J. Paul Attfield,^{||} and Amparo Fuertes^{*,†}

Institut de Ciència de Materials de Barcelona (CSIC), Campus U.A.B., 08193 Bellaterra, Spain, Instituto de Ciencia de Materiales, Universidad de Valencia, P.O. Box 22085, 46071 Valencia, Spain, and Centre for Science at Extreme Conditions and School of Chemistry, University of Edinburgh, King's Buildings, Mayfield Road, Edinburgh EH9 3JZ, United Kingdom

Received October 4, 2007

Revised Manuscript Received December 22, 2007

Nitrogen doping is an important method for modifying the properties of oxides, for example, in tuning the bandgap of the photocatalyst TiO₂ from the UV to the visible region.¹ Stoichiometric oxynitrides can also have useful optical properties such as photocatalytic TaON and yellow-red pigments in the solid solution series CaTaO₂N–LaTaO₂N.^{2,3} Incorporation of nitrogen into ZrO₂ has been reported as an alternative method for cation doping that increases the anion vacancy concentration and stabilizes the cubic or tetragonal form at room temperature.⁴ The resulting materials show good mechanical, catalytic, and optical properties and have been reported as superionic conductors.^{5,6} Ceria (CeO₂) also finds important technological applications such as electrolytes in solid oxide fuel cells and oxygen storage components in automotive three-way and other catalysts,⁷ but nitrogen doping of this key material has not been reported. Here we show that up to 4.5 mol % N can be introduced into ceria under reducing conditions between 550 and 900 °C through ammonolysis.⁸

The oxide ion-conducting and catalytic properties of CeO₂ derive from its fluorite-type structure and the partial reduction of Ce⁴⁺ to Ce³⁺ which leads to the creation of oxide vacancies

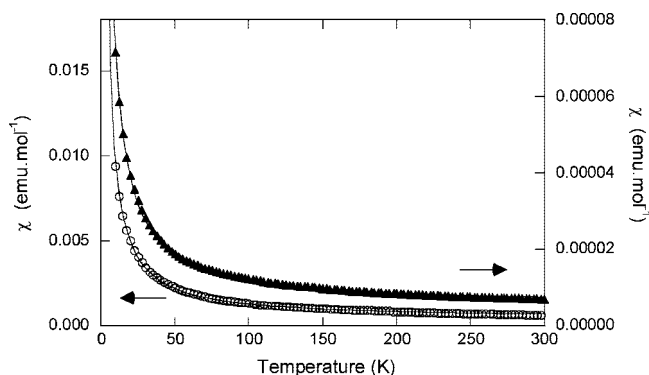


Figure 1. Magnetic susceptibility plots for ceria samples nitrated at 600 °C (triangles, right-hand scale, $y = 0.8\%$ Ce³⁺) and 800 °C (circles, left-hand scale, $y = 11.4\%$ Ce³⁺) showing fits of the equation $\chi = yC/T + \text{Constant}$, where $C = 0.81 \text{ emu} \cdot \text{K} \cdot \text{mol}^{-1}$ is the Curie constant for Ce³⁺.

in bulk, doped, and nanostructured ceria.⁹ CeO₂ is reduced to Ce₂O₃ by heating at 1000 °C under hydrogen gas. The only binary cerium nitride is rocksalt type CeN, although oxide doped materials CeN_{1-x}O_x with rock salt-based superstructures have been reported up to $x = 0.5$.¹⁰ A ternary phase showing similar cell parameters to Ce₂O₃, Ce₂N₂O, has been prepared by heating a mixture of CeN and CeO₂ at 1040 °C in vacuum,¹¹ but nitride-doped CeO₂ has not been produced by this or other methods. Nitride substitution for oxide in CeO₂ will create anion vacancies (V) as CeO_{2-(3x/2)N_xV_{x/2}} and any accompanying reduction of Ce⁴⁺ to Ce³⁺ will increase the vacancy concentration as Ce⁴⁺_{1-y}Ce³⁺_yO_{2-(3x/2)-(y/2)N_xV_{(x+y)/2}}. We have found that both x and y can be varied by heating CeO₂ under flowing ammonia at high temperatures.

Powder samples of CeO₂ (Aldrich, 99.995%) were treated in flowing NH₃ (Carbueros Metálicos, 99.9%) at a rate of 270 cm³/min and temperatures between 400 and 1100 °C during 17 h and were subsequently quenched to room temperature in the ammonia atmosphere. The samples were susceptible to air oxidation because of the presence of Ce³⁺, and they were handled in an Ar-filled glovebox for subsequent characterization. However, their nitrogen content did not change after air exposure.

N contents (x) were determined by combustion analysis (Carlo Erba Instrument), and Ce³⁺ contents (y) were found by fitting the Curie contribution to the magnetic susceptibility. This was measured in a 1 T field at 4–300 K using a Quantum Design SQUID magnetometer. Fits to the susceptibility give Ce³⁺ contents ranging from 0.8 to 18%; representative data are shown in Figure 1. The resulting

* To whom correspondence should be addressed. E-mail: amparo.fuertes@icmab.es.

[†] Institut de Ciència de Materials de Barcelona.

[‡] Present address: Centro de Investigación en Nanociencia y Nanotecnología, (CIN2-CSIC), Edificio CM7, Campus UAB, 08193 Bellaterra (Spain).

[§] Universidad de Valencia.

^{||} University of Edinburgh.

(1) Asahi, R.; Morikawa, T.; Ohwaki, T.; Aoki, K.; Taga, Y. *Science* **2001**, 293, 269.

(2) Hitoki, G.; Takata, T.; Kondo, J. N.; Hara, M.; Kobayashi, H.; Domen, K. *Chem. Commun.* **2002**, 1698.

(3) Jansen, M.; Letschert, H. P. *Nature* **2000**, 404, 980.

(4) Cheng, Y.; Thompson, D. P. *J. Am. Ceram. Soc.* **1993**, 76, 683.

(5) Wendel, J.; Lerch, M.; Laqua, W. *J. Solid State Chem.* **1999**, 142, 163.

(6) Lee, J.; Lerch, M.; Maier, J. *J. Solid State Chem.* **2006**, 179, 270.

(7) (a) Inaba, H.; Tagawa, H. *Solid State Ionics* **1996**, 83, 1. (b) Feng, X. D.; Sayle, D. C.; Wang, Z. L.; Paras, M. S.; Santora, B.; Sutorik, A. C.; Sayle, T. X. T.; Yang, Y.; Ding, Y.; Wang, X. D.; Her, Y. S. *Science* **2006**, 312, 1504. (c) Deluga, G. A.; Salge, J. R.; Schmidt, L. D.; Verykios, X. E. *Science* **2004**, 303, 993. (d) Corma, A.; Atienzar, P.; García, H.; Chane-Ching, J. Y. *Nat. Mater.* **2004**, 3, 394.

(8) Fuertes, A.; Jorge, A. B. Patent Application number 200700482, Spanish Patent and Trademark Office, Spain, February 2007.

(9) (a) Zhou, K.; Yang, Z.; Yang, S. *Chem. Mater.* **2007**, 19, 1215. (b) Wu, L.; Wiesmann, H. J.; Moodenbaugh, A. R.; Klie, R. F.; Zhu, Y.; Welch, D. O.; Suenaga, M. *Phys. Rev. B* **2004**, 69, 125415. (c) Esch, F.; Fabris, S.; Zhou, L.; Montini, T.; Africh, C.; Fornasiero, P.; Comelli, G.; Rosei, R. *Science* **2005**, 309, 752. (d) Shah, P. R.; Kim, T.; Zhou, G.; Fornasiero, P.; Gorte, R. J. *Chem. Mater.* **2006**, 18, 5363. (e) Jobbágy, M.; Mariño, F.; Schönbrod, B.; Baronetti, G.; Laborde, M. *Chem. Mater.* **2006**, 18, 1945. (f) Dutta, P.; Pal, S.; Seehra, M. S.; Shi, Y.; Eyring, E. M.; Ernst, R. D. *Chem. Mater.* **2006**, 18, 5144. (10) Brown, R. C.; Clark, N. J. *J. Inorg. Nucl. Chem.* **1974**, 36, 1777. (11) Barker, M. G.; Alexander, I. C. *J. Chem. Soc., Dalton Trans.* **1974**, 2166.

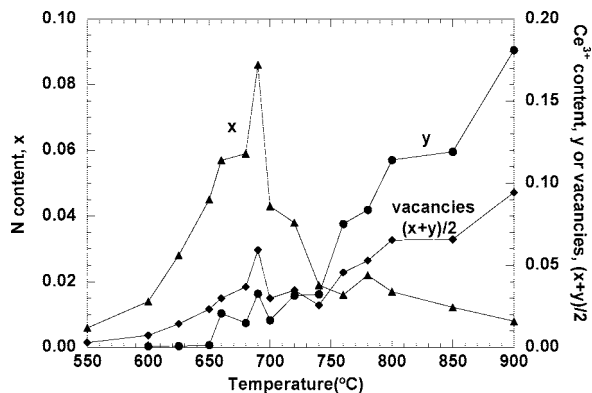


Figure 2. Variation of nitrogen (x), trivalent cerium (y), and anion vacancy $((x+y)/2)$ contents in $\text{Ce}^{4+}_{1-y}\text{Ce}^{3+}_y\text{O}_{2-(3x/2)-(y/2)}\text{N}_x\text{V}_{(x+y)/2}$ with the treatment temperature in ammonia.

stoichiometries (Figure 2) show that nitrogen incorporation in ceria takes place between 550 and 900 °C and is largest in a narrow temperature range with maximum uptake close to 700 °C. The nitrogen content rises rapidly from $x = 0.015$ at 600 °C to 0.09 at 690 °C but falls below 0.02 above 740 °C. The samples prepared at temperatures below 550 °C or higher than 900 °C do not contain nitrogen. The maximum nitrogen uptake in CeO_2 is similar to that obtained in TiO_2 (anatase) porous thin films by treatment in NH_3 , where the introduction of nitrogen starts at 500 °C and increases up to 0.1 mol per formula at 600 °C.¹²

The Ce^{3+} contents in Figure 2 show that cerium is reduced from above 650 °C but the amount of Ce^{3+} increases significantly above 750 °C, up to a maximum of $y = 0.18$ at 900 °C. The concomitant decrease in the nitrogen content above 700 °C suggests competition between the nitriding and reduction processes. Treatments using different flow rates and longer reaction times were performed to investigate the effects of these factors. In experiments with different reaction times (17, 45 and 60 h) performed for some of the samples (e.g., $x=0.04$), x did not change with the reaction time, showing that equilibrium is reached quickly at a given flow rate. Increasing the ammonia flow rate was more significant as this was found to increase the nitrogen uptake (e.g., in samples treated at 700 °C, $x = 0.030$ for a flow rate of 140 cm^3/min , $x = 0.043$ for 270 cm^3/min and $x = 0.065$ for 500 cm^3/min).

The samples are light gray in color for treatments between 600 and 625 °C and darken with increasing treatment temperature (and Ce^{3+} content) to gray for 640–690 °C, light blue for 700–750 °C, dark blue for 760–850 °C and black for the sample prepared at 900 °C. The average number of vacancies, shown in Figure 2 as $(x+y)/2$, reaches a maximum concentration in the 900 °C sample with 0.095 vacancies per mole of cerium. In comparison, the treatment of anatase in NH_3 at temperatures above 700 °C leads to the reduction of Ti^{4+} and the formation of TiN or the solid solution $\text{TiN}_{1-x}\text{O}_x$.^{12,13} However, zirconia forms the solid solution

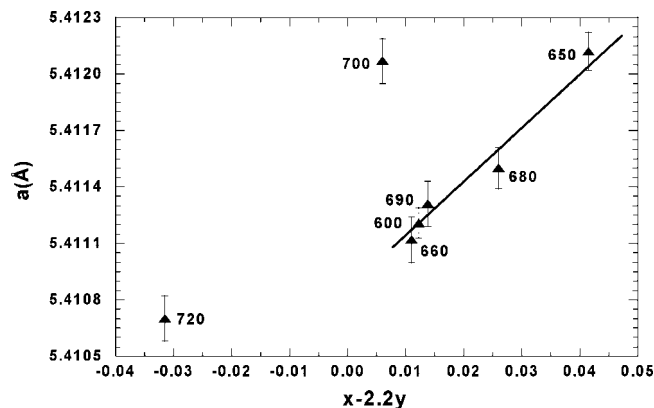


Figure 3. Dependence of a parameter with $x-2.2y$, where x is the nitrogen content and y the trivalent cerium in the solid solution $\text{Ce}^{4+}_{1-y}\text{Ce}^{3+}_y\text{O}_{2-(3x/2)-(y/2)}\text{N}_x\text{V}_{(x+y)/2}$.

$\text{ZrO}_{2-(3x/2)}\text{N}_x\text{V}_{x/2}$ ($0 \leq x \leq 2/7$)¹⁴ as well as three stoichiometric oxynitrides $\text{Zr}_7\text{O}_{11}\text{N}_2$, $\text{Zr}_7\text{O}_8\text{N}_4$ and Zr_2ON_2 , in which Zr^{4+} is not reduced under ammonolysis conditions.

All of the nitrated CeO_2 samples obtained up to 780 °C appear to contain a single cubic $\text{Fm}\bar{3}\text{m}$ phase by powder X-ray diffraction. The lattice parameters were obtained by Le Bail fitting using the program Fullprof.¹⁵ These vary between $a = 5.4107(1)$ and $5.4127(1)$ Å but there is no simple dependence on treatment temperature. a is found to increase with x , showing that the substitution of O^{2-} (4-coordinate radius = 1.38 Å)¹⁶ by N^{3-} (1.46 Å) overcompensates for the volume reduction caused by vacancy formation. However, a decreases with y , indicating that the reduction of Ce^{4+} (8-coordinate radius 0.97 Å) to Ce^{3+} (1.14 Å) is outweighed by the contracting effect of vacancy formation (this may reflect local clustering of vacancies around Ce^{3+} ions). The cubic lattice parameter shows a linear correlation with an optimized combination of the chemical variables, $x-2.2y$ (Figure 3), for samples prepared at temperatures up to 690 °C (where the N content is greatest). Samples prepared at temperatures 700–780 °C do not follow a simple lattice parameter trend and show broader peaks indicating that the distribution of N and anion vacancies is inhomogeneous. Above 800 °C the low symmetry material $\text{CeO}_{1.78}$ ^{17,18} is formed together with the cubic phase, and above 900 °C, vacancy-ordered Ce_7O_{12} predominates with $\text{CeO}_{1.78}$ and the cubic phase is also observed in the X-ray patterns.

High resolution X-ray photoelectron spectroscopy (XPS) measurements performed on a sample treated at 650 °C ($x = 0.045$) and deposited on a conducting tape show evidence of Ce–N bonding. From the experimental N 1s line shape (Figure 4) two contributions are identified with binding energies of 400.1 ± 0.2 and 397.4 ± 0.2 eV, respectively. The 400.1 eV contribution corresponds to molecularly chemisorbed nitrogen ($\gamma\text{-N}_2$) at the surface, as observed in

- (12) Martínez-Ferrero, E.; Sakatani, Y.; Boissière, C.; Grosso, D.; Fuentes, A.; Fraxedas, J.; Sanchez, C. *Adv. Funct. Mater.* **2007**, *17*, 3348.
(13) Chen, H.; Nambu, A.; Wen, W.; Graciani, J.; Zhong, Z.; Hanson, J. C.; Fujita, E.; Rodriguez, J. A. *J. Phys. Chem. C* **2007**, *111*, 1366.

- (14) (a) Gilles, J. C. *Bull. Soc. Chim. Fr.* **1962**, *22*, 2118. (b) Collongues, R.; Gilles, J. C.; Lejus, A. M.; Perez, M.; Jorba, Y.; Michel, D. *Mater. Res. Bull.* **1967**, *2*, 837.
(15) Fullprof 2000. See <http://www-llb.cea.fr/fullweb/powder.htm>. Rodríguez-Carvajal, J. *Physica B* **1993**, *192*, 55.
(16) Shanon, R. D. *Acta Crystallogr., Sect. A* **1976**, *32*, 751.
(17) Bevan, D. J. M.; Kordis, J. J. *Inorg. Nucl. Chem.* **1964**, *26*, 1509.
(18) Brauer, G.; Gingerich, K. A. *J. Inorg. Nucl. Chem.* **1960**, *16*, 87.

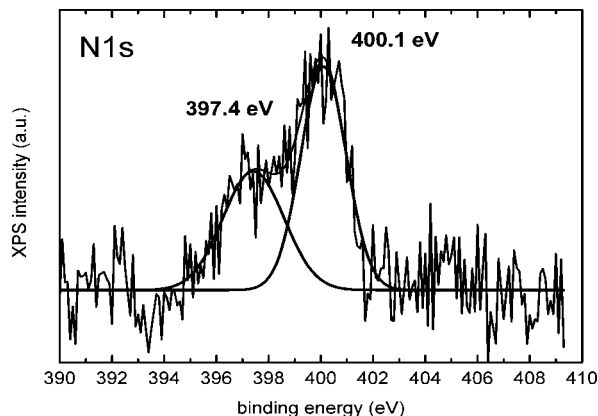


Figure 4. Room temperature XPS spectra of the N 1s line of $\text{CeO}_{1.92}\text{N}_{0.05}\text{V}_{0.025}$, obtained in NH_3 at 650 °C. The continuous lines correspond to a least-squares fit (Gaussians).

N-doped TiO_2 and TiN ,^{1,12,19} while the 397.4 eV contribution is assigned to the formation of Ce–N bonds. Binding energies in the 396–397 eV range are found for nitrides of transition metals, and the only previous report of binding energies in CeN thin films gives a value of 396.2 eV.²⁰ Measurements of samples prepared at higher temperatures showed the presence of Ce^{3+} from the XPS Ce 3d lines.

The nitrified ceria samples have also been analyzed by Raman scattering. CeO_2 has two IR active modes, a doubly degenerate E_u mode at 272 cm^{-1} and a nondegenerate A_u mode at 595 cm^{-1} , and one Raman active mode, a triply degenerate T_{2g} mode, at 465 cm^{-1} ,²¹ although the frequency and width of this mode varies with particle size.^{21,22} Figure 5a shows a typical Raman spectrum for a sample prepared at 700 °C, with $x = 0.04$. The allowed T_{2g} mode and the 2TO(X) (transversal optic mode) are observed, following ref 20. The position of the T_{2g} mode is 465.7 cm^{-1} , and the full width of $8.5 \pm 0.5 \text{ cm}^{-1}$ corresponds to an average particle size of around 100–150 nm.²² The intensity of the peak at 465 cm^{-1} decreases with the treatment temperature in ammonia as a consequence of disorder. In Figure 5b we show the Raman spectra of CeO_2 and doped samples prepared at 700 and 900 °C. The peak around 1180 cm^{-1} corresponds to the 2LO(Γ) (longitudinal optic mode),²¹ while the peak around 2100 cm^{-1} is due to the $^2F_{7/2}$ – $^2F_{5/2}$ transition of Ce^{3+} , from the excited 5d state in the conduction band to the 4f state of Ce. This peak energy changes slightly with nitrogen content, in the range 1940–2250 cm^{-1} . The remaining

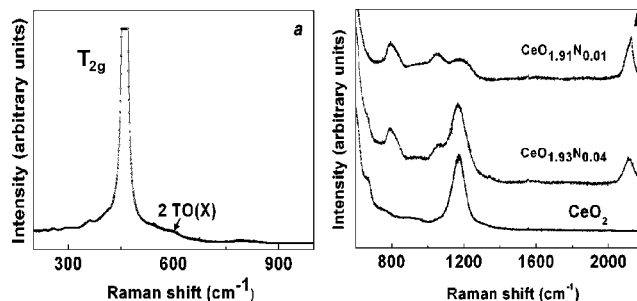


Figure 5. (a) Raman spectrum of $\text{Ce}^{4+}_{0.98}\text{Ce}^{3+}_{0.02}\text{O}_{1.93}\text{N}_{0.04}\text{V}_{0.03}$. The detector is saturated by the Raman active T_{2g} mode to show phonon density of states structure. (b) Raman spectra of CeO_2 and the samples obtained at 700 °C ($\text{Ce}^{4+}_{0.98}\text{Ce}^{3+}_{0.02}\text{O}_{1.93}\text{N}_{0.04}\text{V}_{0.03}$) and 900 °C ($\text{Ce}^{4+}_{0.82}\text{Ce}^{3+}_{0.18}\text{O}_{1.91}\text{N}_{0.01}\text{V}_{0.095}$).

structure in the region below 1000 cm^{-1} is probably phonon density of states. For the sample treated at 900 °C an additional peak is observed at 2250 cm^{-1} that may be due to N_2 occlusion as a result of nitride decomposition at high temperature.¹³

In conclusion, this work shows that incorporation of nitrogen into ceria occurs by treatment in ammonia between 550 and 900 °C, with maximum uptake at temperatures close to 700 °C and with reduction to Ce^{3+} above 650 °C. Chemical analysis and XPS confirm that nitrogen is incorporated in the cubic fluorite-type structure. The solid solution $\text{Ce}^{4+}_{1-y}\text{Ce}^{3+}_y\text{O}_{2-(3x/2)-(y/2)}\text{N}_x\text{V}_{(x+y)/2}$ is formed with $x \leq 0.09$ and $y \leq 0.03$. It is notable that the 650–700 °C region for high nitrogen uptake overlaps with the working range for many ceria-based electrochemical devices, suggesting that nitride may be a significant substitutional defect when ceria is exposed to reducing, nitrogen-rich atmospheres. Nitrogen substitution, together with the presence of Ce^{3+} , may open new possibilities to tune the redox and oxygen storage properties of ceria, relevant to their applications in catalysis and as an electrolyte, and further extends the research horizons for this important material.

Acknowledgment. This work was supported by the Generalitat de Catalunya (Grant 2005SGR 00912), the Ministerio de Educación y Ciencia of Spain (Grant MAT2005-03925), The Royal Society, EPSRC and the Leverhulme Trust, U.K. The Institut de Ciència de Materials de Barcelona and Universidad de Valencia collaborate under the framework of Associated Unit of CSIC “Synthesis and optoelectronics of new materials”. J. Oró-Solé is acknowledged for performing the synthesis of some samples.

Supporting Information Available: Experimental conditions of X-ray diffraction, XPS, and Raman spectroscopy. This material is available free of charge via the Internet at <http://pubs.acs.org>.

CM7028678

(19) Saha, N. C.; Tompkins, H. G. *J. Appl. Phys.* **1992**, 72, 3072.

(20) Xiao, S. Q.; Takai, O. *Thin Solid Films* **1998**, 317, 137.

(21) Webber, W. H.; Hass, K. C.; McBride, J. R. *Phys. Rev. B* **1993**, 48, 178.

(22) Dohcevic-Mitrovic, Z. D.; Scepanovic, M. J.; Grujic-Brojin, M. U.; Popovic, Z. V.; Boskovic, S. B.; Matovic, B. M.; Zinkevich, M. V.; Aldinger, F. *Solid State Commun.* **2006**, 13, 387.